Influence of latent heat and thermal diffusion on the growth of nematic liquid crystal nuclei

B. A. H. Huisman[1] and A. Fasolino[1,2]
[1]*Van 't Hoff Institute for Molecular Sciences, University of Amsterdam, Nieuwe Achtergracht 166, 1018 WV Amsterdam, The Netherlands*
[2]*Theory of Condensed Matter, Institute for Molecules and Materials, Radboud University Nijmegen, Toernooiveld 1, 6525 ED Nijmegen, The Netherlands*
(Received 26 April 2007; published 22 August 2007)

The growth of nematic liquid crystal nuclei from an isotropic melt follows a power law behavior with exponent n found experimentally to vary between $\frac{1}{2}$ for low quench depths, up to 1 for high quench depths. This behavior has been attributed to the competition between curvature and free energy. We show that curvature cannot account for the low quench depth behavior of the nucleus growth, and attribute this behavior to the diffusion of latent heat. We use a multiscale approach to solve the Landau-Ginzburg order parameter evolution equation coupled to a diffusive heat equation, and discuss this behavior for material parameters experimentally measured for the liquid crystal 8CB.

DOI: 10.1103/PhysRevE.76.021706 PACS number(s): 64.70.Md, 61.30.Dk, 81.10.Aj

I. INTRODUCTION

The growth of liquid crystal nuclei from the isotropic melt to an ordered phase has recently been experimentally found to follow a power law with an exponent that gradually changes from $\frac{1}{2}$ to 1 as a function of the quench depth [1]. Here we show that the exponent $\frac{1}{2}$ at low quench depths cannot be due to curvature effects as in domain coarsening [2], but that thermal diffusion of latent heat could account for this behavior.

Nucleus growth is the opposite of domain coarsening, since the coarsening of domains is due to the disappearance of all domains smaller than a typical length scale $L(t)$. For nonconserved fields, like the nematic order parameter, Bray [2] shows that, to decrease the surface energy, a spherical domain shrinks by increasing its curvature $1/R(t)$ as

$$\frac{dR}{dt} = -\frac{C}{R} \Rightarrow R(t) = \sqrt{R(0) - 2Ct}, \tag{1}$$

where C is a positive constant. At time t, all domains that, at $t=0$, were smaller than $R(0)=(2Ct)^{1/2}$ have disappeared, so that the smallest size of the domains gives a typical length scale that grows as $L(t) \propto t^{1/2}$. Bray argues that this growth of the typical length scale can also be described by reversing the sign of the curvature in Eq. (1) as

$$\frac{dL}{dt} = \frac{C}{L} \Rightarrow L(t) \sim t^{1/2}. \tag{2}$$

While this reversed sign macroscopically gives the correct answer for the growth of the typical length scale in domain coarsening of a nonconserved field, Eq. (2) cannot be used to describe the dynamics of a single nematic nucleus. That case is only described by Eq. (1).

Recent experimental work revealed the growth kinetics of nematic nuclei for shallow quenches below the coexistence temperature T_c but well above the spinodal [1,3–6]. Chan and Dierking found experimentally that the growth exponent n describes an S-shaped curve as a function of the quench depth ΔT, between $n=\frac{1}{2}$ close to the coexistence temperature and $n=1$ at deeper quench depths [1]. The exponent $n=1$ at large quench depths is correctly attributed to the free-energy difference between the nematic and isotropic phase, whereas the $n=\frac{1}{2}$, found at shallow quenches, is attributed to curvature effects, by use of Eq. (2), that applies only to the typical length scale in domain coarsening.

Thermal diffusion of latent heat instead, gives a natural explanation of the "diffusive" $n=\frac{1}{2}$ behavior. The latent heat generated during the first-order phase transition heats up the surroundings of the growing phase front, thereby slowing down the nucleus growth. For low quench depths, the motion of the phase front becomes limited by the diffusion of latent heat away from the front, because the front may heat up to the coexistence temperature, where the velocity of the front is zero; this gives rise to $R \sim t^{1/2}$. At deep quenches, the latent heat increases the temperature at the phase front to a constant finite value below the coexistence temperature, so that the front moves at a constant radial velocity, albeit at a lower velocity than without latent heat. We discuss this mechanism to describe nucleus growth in first-order phase transitions in liquid crystals.

The importance of latent heat diffusion for the crystal growth of metals and alloys has been recognized, and a phase field model has been proposed in which an order parameter evolution equation is coupled to a thermal diffusion equation [7]. The authors of this model suggest that this mechanism could be relevant also for weaker first-order transitions, like the isotropic to nematic one in liquid crystals, that are beyond the applicability of their approximations. First, we need to extend their expression of the free energy to allow for quench depths down to the spinodal; second, we need another integration scheme to deal with very broad temperature fields. In fact, in weakly first-order transitions, thermal diffusion is very high, causing a variation of temperature on a length scale much larger than the propagating front. In this case it becomes prohibitive to describe the sharp moving front and the temperature field on the same grid, as is done in Ref. [7]. We propose a multiscale approach that allows us to study the evolution of a nematic nucleus over many more orders of time than conventional phase field methods.

In Sec. II we introduce the coupled differential equations describing the order parameter of the nematic phase and its

TABLE I. Experimentally measured quantities and dimensionless parameters determined from them for the liquid crystal 8CB.

	From Refs. [7,11]		From Eqs. (5) and (6)
M_w	2.92×10^{-1} kg mol^{-1}	τ	2.47×10^{-4} s
ρ_{liq}	9.79×10^{2} kg m^{-3}	η	1.38
T_c	3.13×10^{2} K	p	3.38×10^{-6}
L	6.12×10^{2} J mol^{-1}		
c_p	7.30×10^{2} J mol^{-1} K^{-1}		
σ	9.4×10^{-6} J m^{-2}		
ξ_m	7.1×10^{-9} m		
β	1.0×10^{-4} m s^{-1} K^{-1}		
D_T	6.0×10^{-8} m^2 s^{-1}		

coupling to the temperature field. Here we also discuss the relevant physical parameters. In Sec. III we present our multiscale approach to the solution of the problem set in Sec. II. Details of the calculations are given in Appendixes A and B. In Sec. IV we describe our results for the growth of nematic nuclei over a range of quench depths and their power law behavior. The calculations are done with parameters appropriate for the octylcyanobiphenyl (8CB) liquid crystal. Section V provides a summary and conclusions.

II. ORDER PARAMETER AND COUPLING TO A TEMPERATURE FIELD

The isotropic phase of liquid crystals is characterized by the absence of spatial and orientational order. In the nematic phase orientational order appears. The isotropic to nematic transition is usually described by the following order parameter [8]:

$$m = \frac{3}{2}\left\langle \frac{3\cos^2(\theta)-1}{2} \right\rangle, \tag{3}$$

where θ is the angle between the average orientation of the nematic domain, and the local orientation of the liquid crystal molecules. The prefactor $\frac{3}{2}$ is here introduced for convenience, to be compatible with Ref. [7]. In the isotropic phase $m\equiv 0$, while in a perfectly aligned nematic domain $m=\frac{3}{2}$. We study the dynamics of the order parameter, coupled to a dimensionless temperature field $u(r,t)=c_p(T(r,t)-T_c)/L_c$, where T_c is the coexistence temperature and L_c and c_p are the latent heat and the specific heat at T_c, respectively. Using the notation of Ref. [7], the dimensionless time-dependent Landau-Ginzburg equation for the spatially varying, scalar order parameter $m(r,t)$ coupled to the diffusive heat equation can be written in spherical coordinates as (see also Appendixes A and B)

$$\frac{\partial m}{\partial t} = \frac{1}{2}\left(\frac{\partial^2 m}{\partial r^2} + \frac{d-1}{r}\frac{\partial m}{\partial r}\right) - \frac{\partial f}{\partial m}, \tag{4a}$$

$$\frac{\partial u}{\partial t} = \frac{1}{2p}\left(\frac{\partial^2 u}{\partial r^2} + \frac{d-1}{r}\frac{\partial u}{\partial r}\right) + 2m\frac{\partial m}{\partial t}, \tag{4b}$$

where f is the temperature-dependent free-energy density given below, and d is the dimensionality. The m-dependent term on the right-hand side of Eq. (4b) accounts for the latent heat, caused by the change of entropy, and hence a change in the order parameter, during the transition. The dimensionless parameter p sets the ratio in time and length scales between the order parameter equation and the heat equation. This parameter is defined as

$$p = \frac{\xi_m^2}{D_T}\frac{1}{\tau_m} = \frac{\xi_m^2}{D_T}\left(\sqrt{2}\sigma\frac{M_W}{\rho_c}\frac{T_c}{L_c}\frac{\beta}{\xi_m^2}\right), \tag{5}$$

where ξ_m is the microscopic correlation length and D_T is the diffusivity at T_c. τ_m is a time constant related to the microscopic relaxation of the order parameter, where σ is the surface tension between the two phases at T_c, M_W is the molecular weight, ρ_c is the density at T_c, and β is the kinetic coefficient. All these quantities are known to some extent for 8CB (see Table I), giving a very low value of $p=3.38\times10^{-6}$, which makes a straightforward numerical solution of the coupled equations (4a) and (4b) prohibitive.

In Eqs. (4a) and (4b), time is scaled by τ_m, lengths by $\sqrt{2}\xi_m$, and the free-energy density is scaled by $6\sigma/\xi_m$. The dimensionless free-energy density f (see Fig. 1) is given by a Landau expansion of the free energy around T_c in terms of the order parameter $m(r,t)$ and of the temperature field $u(r,t)$,

$$f = m^2(m-1)^2 + \frac{1}{2}\eta u m^2, \quad \eta = \frac{\xi_m L_c^2 \rho_c}{3\sigma c_p T_c M_W}, \tag{6}$$

where the dimensionless coupling constant η is determined by noting that at T_c, i.e., at $u=0$, the latent heat is given by $L_c = T\Delta S|_{T=T_c}$, where ΔS is the difference in entropy $S=-\partial F/\partial T$ [see Eq. (A1)] between the isotropic ($m=0$) and the nematic ($m=1$ at T_c) phase.

The free-energy density of Ref. [7] is an approximation of Eq. (6), giving the same free energy to first order in u around $u=0$. In contrast to Ref. [7] the order parameter in the disordered phase obtained from Eq. (6) is zero for all temperatures where the disordered phase is metastable, and more importantly the ordered phase is stable down to much larger values of ηu (thin solid gray line versus solid black line in

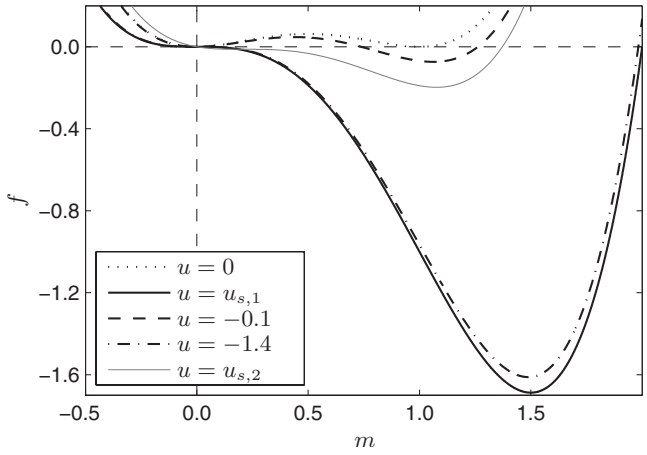

FIG. 1. Free-energy density f from Eq. (6) as a function of the order parameter (OP) m in order of increasing temperature. The dotted line shows the free energy at $u=0$, where both the disordered phase at $m=0$ and the ordered phase at $m=1$ are equally stable. The black solid line shows the free energy at the spinodal temperature $u_{s,1}$, the thin solid gray line shows the free energy used in Ref. [7] at its spinodal temperature $u_{s,2}$. The dashed and dashed-dotted line denote the highest and lowest temperature we use in this paper. Note that the lowest temperature is very close to the spinodal and beyond the reach of the free energy used in Ref. [7].

Fig. 1). As we will discuss later this is especially important for liquid crystals, where $\eta \sim 1$. At these high values of η the approximation of Ref. [7] is already in the spinodal regime for very shallow quenches. Moreover we extend their one-dimensional analysis to the case of a d-dimensional sphere, so that we can also study the effect of curvature in two and three dimensions and address the claim that curvature causes the exponent to approach $n=\frac{1}{2}$ at shallow quenches.

III. MULTISCALE APPROACH

As was briefly mentioned in the preceding section, the low value of p in Eq. (4b), prohibits a numerical integration of the coupled equations. Because of this large scale difference Eqs. (4a) and (4b) cannot be integrated numerically by the usual integration methods as the grid spacing Δr must be small enough to resolve the spatial detail of the interface region, and the time step must be of order $\Delta t \sim p(\Delta r)^2$ [9], which is prohibitively small compared to the times and lengths we are interested in. To solve this problem we have devised a multiscale numerical approach that allows to study the evolution of the nucleus over many more orders of time than conventional methods.

Our approach uses the fact that Eq. (4a) can be solved analytically [10], if we assume a shape preserving profile. From Eq. (6), the value of the order parameter m_o in the ordered phase is

$$m_o = \tfrac{3}{4} + \tfrac{1}{4}\sqrt{1 - 4\eta u}, \tag{7}$$

so that the analytical solution of Eq. (4a) (see Appendix A) provides the steplike shape of the order parameter profile as

$$m(r) = \frac{m_o}{2}(1 - \tanh\{m_o[r - R(t)]\}), \tag{8}$$

as well as its interface velocity $\dot{R}(t)$,

$$\dot{R}(t) = v\left(1 - \frac{R_c}{R(t)}\right), \quad R_c = \frac{d-1}{2v}, \quad v = 3(m_o - 1), \tag{9}$$

where R_c is the critical nucleus size below which a nucleus does not grow, and v is the (asymptotic) velocity of the nucleus at a temperature u. Equation (9) becomes equal to Eq. (1) at the coexistence temperature $u=0$, since there is no free-energy difference between the domain and its surroundings, causing all domains to shrink, because $R_c=\infty$. By using Eq. (2) to describe the increase of the typical length scale in domain coarsening, and adding a free-energy difference driving nucleus growth, Ref. [1] derives an expression similar to Eq. (9), albeit with an opposite sign of the curvature term $[1/R(t)]$. Its solution contains a regime, whose duration increases for decreasing free-energy difference, where the growth exponent equals $n=\frac{1}{2}$, before ultimately reaching $n=1$ for all quench depths. It is this transient $n=\frac{1}{2}$ regime becoming more and more prominent at shallower quenches, that is used to explain the S-shaped curve of the growth exponent as a function of free energy and hence quench depth. In nucleus growth however, a decreasing curvature implies a larger nucleus and hence more surface energy, making curvature oppose, not contribute to, the growth of a domain. Equation (9) does not contain an $n=\frac{1}{2}$ regime, eliminating curvature as the cause of the experimentally measured $n=\frac{1}{2}$ exponent.

Although in principle the temperature field is not uniform, nor time independent, the temperature field can be treated as uniform over the width of the interface for low values of p. In this case Eqs. (8) and (9) are still valid at time t if the temperature at the phase front position $u=u(R,t)$ is used to calculate $v=v(R,t)$ and $m_o=m_o(R,t)$. Then $\dot{R}(t)$ can be determined at each time step, and numerically integrated to obtain $R(t)=R_0+\int_0^t \dot{R}(t)dt$. The latent heat term on the right-hand side of Eq. (4b) is also known at time t, and resembles a Gaussian around $R(t)$, with a width much smaller than the spatial variations in the temperature field. The latent heat can be described as a Dirac δ function $\delta(R)$ at $R(t)$, multiplied by a constant (see Appendix B),

$$2m(r,t)\frac{\partial m(r,t)}{\partial t} \approx \delta(R)\dot{R}(t)\left(1 + \frac{v(R,t)}{3}\right)^2, \tag{10}$$

so that Eqs. (4a) and (4b) become

$$\frac{\partial R}{\partial t} = v - \frac{d-1}{2R} \quad \text{with } v = \frac{3}{4}[\sqrt{1 - 4\eta u(R)} - 1], \tag{11a}$$

$$\frac{\partial u}{\partial t} = \frac{1}{2p}\left(\frac{\partial^2 u}{\partial r^2} + \frac{d-1}{r}\frac{\partial u}{\partial r}\right) + \frac{\partial R}{\partial t}\left(1 + \frac{v}{3}\right)^2 \delta(R). \tag{11b}$$

In practice we determine the temperature $u(R)$ at the phase front $R(t)$ by interpolating the temperature field, and use it to calculate the phase front velocity $\dot{R}(t)$ from Eq. (9)

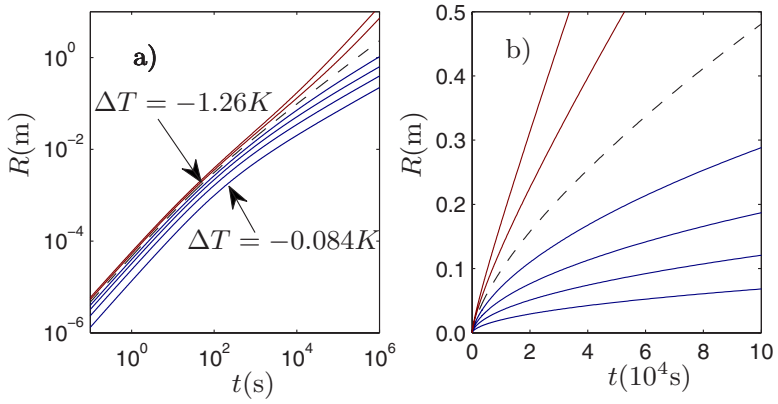

FIG. 2. (Color online) Radius $R-R_0$ of a spherical nucleus as a function of time t, for increasing quench depth $\Delta T=u_{\mathrm{quench}}L_c/c_p$: $\Delta T=-0.084$ K, -0.2415 K, -0.42 K, -0.59 K, -0.75 K, -0.92 K, -1.1 K, and -1.26 K. In (a) the data is displayed on a log-log scale plot to reveal the growth exponent, whereas (b) shows the same data linearly on a time scale where the two growth regimes diverge. Parameters are taken from Table I. The dashed line denotes the temperature $u_{\mathrm{quench}}=-1$, $(\Delta T=-L_c/c_p)$. Lines below the dashed line (blue in online version) denote shallow quenches where $\lim_{t\to\infty} R\propto t^{1/2}$, lines above the dashed line (red in online version) denote deep quenches where $\lim_{t\to\infty} R\propto t^1$.

and the latent heat integrated over space from Eq. (10) analytically at each time t. The latent heat is then injected into the heat equation as a δ pulse at position $R(t)$. The temperature field is then calculated at the next time step by integrating the heat equation numerically using Crank-Nicolson integration [9], and we use $\dot{R}(t)$ to propagate the phase front by using a second-order integration scheme.

By solving the shape and evolution of the order parameter profile analytically at constant temperature, we have eliminated the smallest length scale from the coupled equations, and can focus on the length scale of the temperature field instead. As the temperature field widens with time, we can increase the grid spacing, and thereby also increase the time step during the numerical integration of the heat equation.

We employ an equidistantly spaced dimensionless temperature grid over the radial coordinate r, fixed at the highest value of r to u_{quench} and mirrored at the origin; initially the entire temperature field is set to u_{quench}. We start with a nucleus with a radius $R_0=10R_c^{3\mathrm{D}}$, where $R_c^{3\mathrm{D}}$ is the critical nucleus size in three dimensions also for the one-dimensional (1D) planar nucleus where $R_c=0$. The initial grid spacing is $\Delta r=R_0/5$ and time is spaced by $\Delta t=4p(\Delta r)^2$. As the nucleus grows, we coarsen and widen the grid automatically to describe the temperature field around the interface with enough, but not excessively high detail.

IV. RESULTS

In this section we present the results for the temporal behavior of the nucleus size for a range of quench depths and discuss its power law behavior. Although we do not have experimental data on nucleus growth in 8CB, it is the only liquid crystal for which all the parameters have been measured or estimated.

Qualitatively our results are in agreement with the experimental findings, for the bent core liquid crystal molecules studied by Chan and Dierking [1]. However, to our knowledge the liquid crystal 8CB is the only one for which all parameters needed for our model have been measured or estimated. When using the parameters for 8CB we find that the experimentally found S-shaped curve can only be reproduced for too large nuclei. We discuss this point at the end of this section.

In Fig. 2 the radius $R-R_0$ of a growing spherical nucleus is shown for different values of the quench depth $\Delta T=(T-T_c)=L_c u_{\mathrm{quench}}/c_p$. The initial behavior of the growth is similar for all quench depths and is linear in time, until the curves separate into two qualitatively different regimes. From the plots on a logarithmic scale [Fig. 2(a)] one can see that the two regimes are characterized by different exponents of the power law. For quench depths $-L_c/c_p<\Delta T<0$ the radius approaches $R\sim t^{1/2}$ asymptotically, whereas for $\Delta T<-L_c/c_p$ the radius approaches $R\sim t^1$.

As shown in Fig. 3(a), for large quench depths $\Delta T<-L_c/c_p$ the latent heat increases the temperature of the front to a constant, finite temperature below T_c $(u=0)$; as the temperature at the front approaches a constant value, the velocity approaches a constant value as well. For small quench depths $-L_c/c_p<\Delta T<0$ [Fig. 3(b)], the temperature at the front approaches the coexistence temperature. The velocity of the front is then limited by the diffusion of heat away from the front, and it is this diffusion process that scales as $R\sim t^{1/2}$.

In Fig. 4 we show the growth exponent n determined for three different regimes in one, two, and three dimensions. To this purpose we perform a linear least-squares fit of our results for $R(t)$, spaced equidistantly on a logarithmic time scale, as $\ln\{[R(t)-R_0]/R_0\}=n\ln(t/t_0)+c$, where $t_0=1$ s. For long times $t>10^3$ s, where the radii are large, we obtain an S-shaped curve between $n=1/2$ at $\Delta T\lesssim 0$ and $n=1$ at $\Delta T\ll -L/c_p$. If the exponent is evaluated on a shorter radial range, the S-shaped curve becomes less pronounced. Note that the asymptotic qualitative behavior does not depend on the dimension of the nucleus, although it takes longer to be reached for higher dimensional nuclei. The S-shaped curve is even observed for a flat surface with zero curvature. At the onset of the long time behavior the radii are many orders of

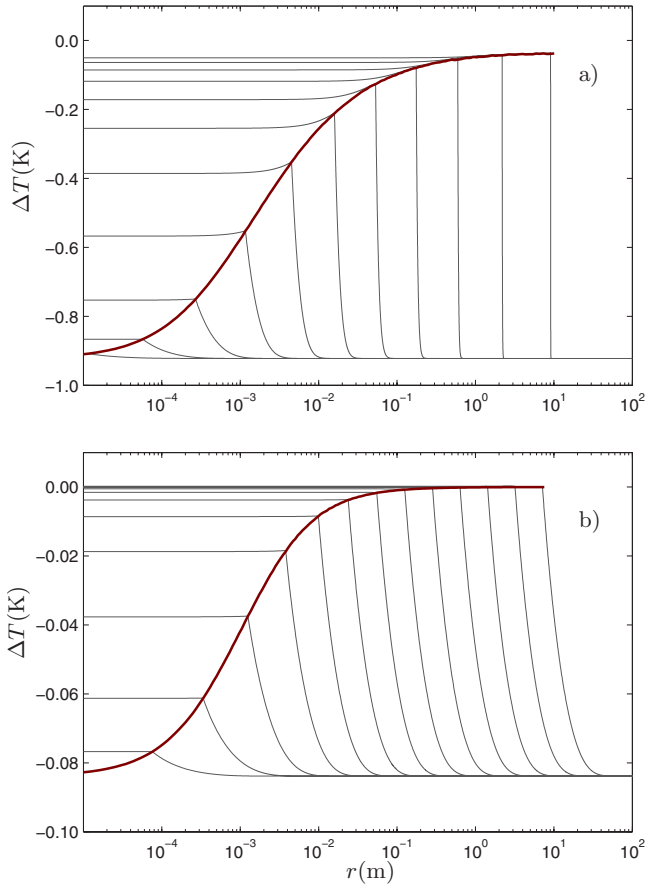

FIG. 3. (Color online) Thin lines: Temperature field $\Delta T(r)$ at a given time during the growth of a three-dimensional nucleus for two temperatures. The profiles are shown from left to right at exponentially increasing intervals of time, $t_n = t_0 5^n$. The thick line is the temperature $\Delta T(R(t))$ at the interface position $R(t)$. In (a) the isotropic phase is quenched to $\Delta T = -0.92\ \mathrm{K} < -L_c/c_p$, at which a nucleus will grow as $R \propto t^1$ asymptotically. In (b) the isotropic phase is quenched to $\Delta T = -0.084\ \mathrm{K} > -L_c/c_p$, at which $R \propto t^{1/2}$ asymptotically. In (a) the first profile is taken at $t = 0.2$ s and the last at $t = 2 \times 10^6$ s. In (b) the first profile is taken at $t = 10$ s and the last at $t = 2 \times 10^9$ s. Parameters are taken from Table I.

magnitude larger than the critical nucleus size, hence curvature does not play any role at this stage.

The curve of Fig. 4 is similar to the experimental data of Chan and Dierking [1], although the long time behavior is reached at larger radii and times than reported in that experiment. The radii at which this long time behavior sets in are determined by ξ, p, and η of Eqs. (5) and (6). As noted in Ref. [7] the values of ξ and β are poorly measurable or can only be estimated. We have found that the radii at which the long time behavior starts, scale linearly with p^{-1} and ξ for small values of p. For our simulations to match the experimental time and length scales, p should be one to two orders of magnitude larger.

Both τ and p depend on seven experimentally measurable quantities, and both parameters have only been estimated for the isotropic to nematic transition in 8CB [7,11]. It is unknown whether the growth exponent of 8CB follows an S-shaped curve as reported by Chan and Dierking for bent core molecules, or whether the parameters (Table I) are applicable to the liquid crystal transition studied by them [1]. Moreover, the parameters for 8CB that we have used are measured or estimated for the weakly first-order isotropic to nematic phase transition, whereas the experimentally studied transition is first order. Therefore, it may be expected that latent heat dominates even more in the latter case. All these considerations lead us to believe that the uncertainty of the parameters causes the difference between the length scales of the experiments and Fig. 4, and that the diffusion of latent heat is crucial to account for the experimental findings. Our mechanism implies a crossover from $n = \frac{1}{2}$ to $n = 1$ at $\Delta T = -L_c/c_p$. A stringent experimental confirmation of our conjecture would therefore require the crossover value of the quench depth to coincide with the ratio of L_c and c_p obtained by independent measurements.

Although the reduction of curvature plays a key role in domain coarsening, in spherical growth reducing the curvature means increasing the nucleus size and therefore its interface area. Curvature in a spherical growth model therefore acts to decrease the nucleus size, illustrated by the negative sign of the curvature term $[-vR_c/R(t)]$ in Eq. (9), not increase it as in Eq. (4) of Ref. [1]. If thermal diffusion causes the $n = \frac{1}{2}$ behavior for shallow quenches $-L_c/c_p < \Delta T < 0$, the diffusive effect should become stronger with time, i.e., the growth exponent should approach $n = \frac{1}{2}$ from above, while if the behavior was due to curvature, its effect should subside for larger radii and longer times and evolve towards $n = 1$.

V. SUMMARY AND CONCLUSIONS

In this paper we have shown that the diffusion of latent heat away from a growing nematic nucleus slows down its

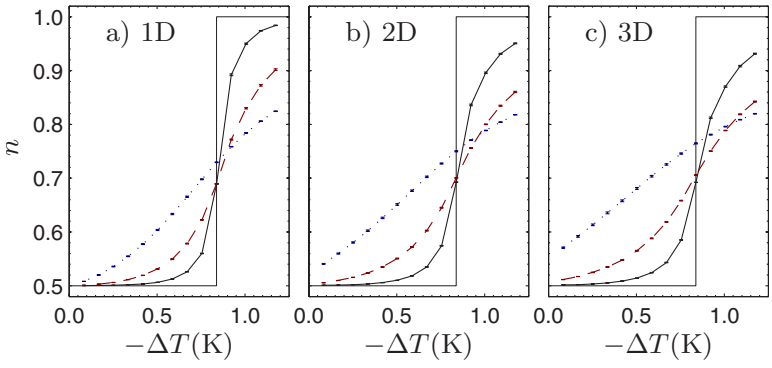

FIG. 4. (Color online) Exponent n found by least-squares fitting of the data of Fig. 2 to $(R - R_0) \propto t^n$, as a function of quench depth $-\Delta T$, where the negative sign is introduced to be compatible with Ref. [1]. The dotted (blue, online) line is n fitted for radii $10^{-5}\ \mathrm{m} < R(t) < 10^{-3}\ \mathrm{m}$, the dashed (red, online) line is a fit for $10^{-4}\ \mathrm{m} < R(t) < 10^{-2}\ \mathrm{m}$, and the solid (black, online) line for $10^{-3}\ \mathrm{m} < R(t) < 10^{-1}\ \mathrm{m}$. The thin solid line denotes the asymptotic value of n: (a) one dimension, (b) two dimensions, (c) three dimensions.

growth, and causes the growth exponent to reach $n=\frac{1}{2}$ for quenches above $T^*=T_c-L/c_p$. Moreover, diffusion of latent heat causes a transient regime, so that the value $n=1$ for $T<T^*$ is reached only asymptotically. Therefore, measuring the growth exponent for limited times and radii yields an S-shaped curve for the exponent as a function of quench depth. This curve is qualitatively similar to what is experimentally measured [1], although the time and length scales are rather different. This discrepancy can be either related to the different liquid crystals examined in experiment and studied here, or to the uncertainty in the parameters used in our calculations.

Conversely we have shown that the explanation, borrowed from the theory of domain coarsening, attributing the S-shaped curve to the competition between curvature at low quenches and the free-energy difference at high quenches, does not apply to nucleus growth. Our results challenge the current belief that latent heat is not relevant at the isotropic to nematic phase transition, because of the relatively high thermal diffusivity in these compounds. However, since the curvature mechanism cannot provide an alternative explanation for the $n=\frac{1}{2}$ limit, our conjecture deserves serious consideration. The experimental test we propose at the end of Sec. IV could resolve this issue.

ACKNOWLEDGMENTS

This work is a part of the research programme of the "Stichting voor Fundamenteel Onderzoek der Materie (FOM)," which is financially supported by the "Nederlandse Organisatie voor Wetenschappelijk Onderzoek (NWO)."

APPENDIX A: SHAPE AND VELOCITY OF THE ORDER PARAMETER PROFILE

The dimensionless time-dependent Landau-Ginzburg equation for order parameter evolution is given by

$$\frac{\partial m}{\partial t}=-\frac{\delta F}{\delta m},\quad F=\int\left(\frac{1}{2}(\nabla m)^2+f\right)dV \tag{A1}$$

with m the order parameter field and f the local free-energy density. Functional derivation of the free energy in Eq. (A1) gives, for a d-dimensional spherical symmetry,

$$\frac{\partial m}{\partial t}=\frac{1}{2}\frac{\partial^2 m}{\partial r^2}+\frac{d-1}{2r}\frac{\partial m}{\partial r}-\frac{\partial f}{\partial m}. \tag{A2}$$

Initially we assume that the temperature u is constant over the whole system. Furthermore, we assume that the order parameter profile of a growing nucleus of size $R(t)$, only varies in the neighborhood of $R(t)$. With these assumptions Eq. (A2) becomes

$$\frac{\partial m}{\partial t}=\frac{1}{2}\frac{\partial^2 m}{\partial r^2}+\frac{d-1}{2R(t)}\frac{\partial m}{\partial r}-\frac{\partial f}{\partial m}. \tag{A3}$$

By changing variables $s=r-R(t)$ we move to a frame with the velocity $\dot{R}(t)$ of the phase front and rearrange terms to give

$$\frac{1}{2}\frac{\partial^2 m}{\partial s^2}+\left(\frac{d-1}{2R(t)}+\frac{\partial R(t)}{\partial t}\right)\frac{\partial m}{\partial s}-\frac{\partial f}{\partial m}=0. \tag{A4}$$

We assume a shape preserving profile, meaning that Eq. (A4) should be independent of time. This is the case when

$$\dot{R}=\frac{\partial R}{\partial t}=v-\frac{d-1}{2R(t)}=v\left(1-\frac{R_c}{R(t)}\right),\quad R_c=\frac{d-1}{2v}, \tag{A5}$$

where v is a constant to satisfy the time independence of Eq. (A4) and R_c is the critical nucleus size, known from classical nucleation theory.

Combining Eqs. (A4) and (A5) gives a second-order ordinary differential equation (ODE) in s,

$$\frac{1}{2}\frac{\partial^2 m}{\partial s^2}+v\frac{\partial m}{\partial s}=\frac{\partial f}{\partial m}, \tag{A6}$$

which can be cast into two coupled first-order ODE's,

$$\frac{\partial m}{\partial s}=y,$$

$$\frac{\partial y}{\partial s}=2\frac{\partial f}{\partial m}-2vy. \tag{A7}$$

We divide $\partial y/\partial s$ by y,

$$\frac{1}{y}\frac{\partial y}{\partial s}=\frac{\partial s}{\partial m}\frac{\partial y}{\partial s}=\frac{\partial y}{\partial m}=\frac{2}{y}\frac{\partial f}{\partial m}-2v,$$

and since $\partial f/\partial m$ of Eq. (6) is factorizable into exactly three roots, where m_o is given in Eq. (7), we obtain

$$\frac{\partial y}{\partial m}=\frac{2}{y}4m(m-m_o)(m-3/2+m_o)-2v. \tag{A8}$$

Equation (A8) becomes independent of m if we choose

$$y=2m(m-m_o), \tag{A9}$$

and directly gives the value for v,

$$v=3(m_o-1). \tag{A10}$$

The order parameter profile is found by taking the primitive of $1/y=\partial s/\partial m$, from Eq. (A9),

$$s(m)=\frac{1}{2m_o}\ln\left(1-\frac{m_o}{m}\right)+k, \tag{A11}$$

where k is determined by the definition of $R(t)$. If we choose $0<m(s)<m_o$ and define $R(t)$ as the position where $m(s)|_{s=0}=m_o/2$, then

$$s(m_o/2)=0\Rightarrow k=-\frac{\ln(-1)}{2m_o}, \tag{A12}$$

so that Eq. (A11) becomes

$$s(m)=\frac{1}{2m_o}\ln\left(\frac{m_o}{m}-1\right). \tag{A13}$$

Inverting Eq. (A13) results in the profile

$$m(s) = \frac{m_o}{1 + \exp(2m_o s)}, \tag{A14}$$

$$m(r) = \frac{m_o}{2}(1 - \tanh\{m_o[r - R(t)]\}). \tag{A15}$$

The time derivative of $m(r)$ is given by

$$\frac{\partial m(r)}{\partial t} = \dot{R}(t)\frac{m_o^2}{2}(1 - \tanh\{m_o[r - R(t)]\}^2), \tag{A16}$$

where $\dot{R}(t)$ is given by Eq. (A5).

APPENDIX B: LATENT HEAT

If in a time interval Δt the phase front moves less than its interface width, then the latent heat term in Eq. (4b) can be calculated from Eqs. (A15) and (A16) as

$$\frac{\partial L}{\partial t} = 2m\frac{\partial m}{\partial t} = \frac{\dot{R}(t)m_o^3}{2}(1 - b^2)(1 - b), \tag{B1}$$

where

$$b = \tanh\{m_o[r - R(t)]\}.$$

Equation (B1) resembles a Gaussian around $r=R(t)$, with a width of order m_o^{-2}. If the spatial extent of the latent heat term is negligible compared to the spatial variations of the temperature field, Eq. (B1) can be written as a Dirac δ pulse at $r=R(t)$ multiplied by a constant

$$2m\frac{\partial m}{\partial t} \approx \delta(R)\int_0^\infty 2m\frac{\partial m}{\partial t}dr \approx \delta(R)\int_{-\infty}^\infty 2m\frac{\partial m}{\partial t}dr$$

$$= \delta(R)\dot{R}(t)m_o^2 = \delta(R)\dot{R}(t)(1 + v/3)^2. \tag{B2}$$

Equation (B2) is a good approximation when $R \gg 0$. Note that m_o and v depend on the temperature at $R(t)$.

[1] H. K. Chan and I. Dierking, Phys. Rev. E **70**, 021703 (2004).
[2] A. J. Bray, Adv. Phys. **51**, 481 (2002).
[3] S. Bronnikov and I. Dierking, Phys. Chem. Chem. Phys. **6**, 1745 (2004).
[4] I. Dierking and C. Russell, Physica B **325**, 281 (2003).
[5] I. Dierking, J. Phys. Chem. B **104**, 10642 (2000).
[6] K. Diekman, M. Schumacher, and H. Stegemeyer, Liq. Cryst. **25**, 349 (1998).
[7] H. Löwen, J. Bechhoefer, and L. S. Tuckerman, Phys. Rev. A **45**, 2399 (1992).
[8] P. G. de Gennes and J. Prost, *The Physics of Liquid Crystals*, 2nd ed. (Oxford University Press, Oxford, 1993).
[9] J. Crank and P. Nicolson, Proc. Cambridge Philos. Soc. **43**, 50 (1947).
[10] S. K. Chan, J. Chem. Phys. **67**, 5755 (1977).
[11] J. Bechhoefer, A. J. Simon, A. Libchaber, and P. Oswald, Phys. Rev. A **40**, 2042 (1989).